

parts) are 4080 and 1300 ev, respectively. The total value agrees fairly well with Slotnick and Heitler's figure of 5000 ev and with the 5220 ev²⁴ obtained by Dancoff and Drell. [These values have been re-computed using the choice (56) for the coupling constant.]

²⁴ This figure was incorrectly stated as 6100 ev in the author's letter, *Phys. Rev.* **86**, 434 (1952). The error was pointed out by Dr. Drell in a private communication.

The discrepancies between their results and the 5380 ev can probably be attributed to their having used, in their numerical integrations, slightly different values for the meson-nucleon mass ratio.

This problem was suggested by Professor G. Wentzel, whose advice and encouragement are very gratefully acknowledged. Thanks are also due Dr. M. Goldberger and Dr. M. Gell-Mann for many helpful discussions.

Cross Section and Angular Distribution of the $D(d, p)T$ Reaction*

W. A. WENZEL AND WARD WHALING

Kellogg Radiation Laboratory, California Institute of Technology, Pasadena, California

(Received August 11, 1952)

The $D(d, p)T$ reaction cross section has been measured by two methods using D_2O ice targets. For E_d from 206 to 516 kev, a double-focusing magnetic spectrometer was used to obtain the momentum spectrum of the protons and tritons, from which the reaction cross section can be determined. For E_d from 35 to 550 kev, the proton yield from a thick target was differentiated to obtain the cross section. Both thin and thick target methods were used to measure the angular distribution over the energy range E_d from 35 to 550 kev. The angular distribution is expressed in terms of a Legendre polynomial expansion. Various sources of experimental error are considered and the probable error of the total cross section is found to be ± 5 percent.

I. INTRODUCTION

SINCE the discovery by Lawrence, Lewis, and Livingston¹ in 1933 that two deuterons can react with the emission of long-range protons, the reaction $H^2 + H^2 \rightarrow H^1 + H^3 + 4.032$ Mev has been studied extensively. Although early investigators determined that the yield was large and anisotropic, accurate measurements of the cross section have been possible only in the past few years.²⁻⁶ In attempts to extend the measurements to very low energies, some experimental problems which are minor at higher energies become increasingly troublesome. The use of thin gas targets with differential pumping is subject to uncertainties due to beam neutralization and energy loss. The use of foils introduces straggling in the beam energy and requires an accurate knowledge of the window thickness at each energy at which the reaction is to be studied. The accuracy of the thick solid target measurements has been limited by uncertainties in the stopping cross section, which is needed to obtain the reaction cross section from the thick target yield. Recent measurements in this laboratory⁷ of the stopping cross section of D_2O ice for protons of 18-550 kev enable us to measure the

$D(d, p)T$ cross section by the thick target method with higher accuracy than has been attained previously.

At higher energies, E_d from 206 to 516 kev, the cross section was obtained by another method. A double-focusing magnetic spectrometer was used to measure the yield of protons and tritons from a thick target as a function of their momenta. This spectrum of the emitted particles can be used to determine the "thin target" cross section, and the observation of both protons and tritons provides a check on the internal consistency of the experimental method.

The angular distribution of the reaction was measured by making observations at 10° intervals over the range θ_{lab} from 80° to 150° . Above 200 kev a thin ice target was used, and the yield at each angle relative to a monitor counter at $\theta_{lab} = 70^\circ$ gives the angular distribution. For deuteron energies below 200 kev it was necessary to measure the thick target yield at each angle. The differentiated thick target yield gives $d\sigma/d\Omega$ at each angle.

II. CROSS SECTION MEASURED WITH THE MAGNETIC SPECTROMETER

A double focusing magnetic spectrometer was used to observe particles emitted at an angle of 90.3° with respect to the incident deuteron beam. The D_2O ice target was deposited on a copper surface cooled with liquid nitrogen in a target chamber that has been described previously.⁷ The aperture of the spectrometer was adjusted to subtend a small solid angle, 0.00127 steradian, at the target, in order to obtain high effective resolution. A scintillation counter was used to detect

* Assisted by the joint program of the ONR and AEC.

¹ Lawrence, Livingston, and Lewis, *Phys. Rev.* **44**, 56L (1933).

² Bretscher, French, and Seidl, *Phys. Rev.* **73**, 815 (1948).

³ Blair, Freier, Lampi, Sleator, and Williams, *Phys. Rev.* **74**, 1599 (1948).

⁴ Moffatt, Sanders, and Roaf, *Proc. Roy. Soc. (London)* **212**, 225 (1952).

⁵ Sawyer, Arnold, Phillips, Stovall, and Tuck, *Phys. Rev.* **86**, 583 (1952).

⁶ K. G. McNeill and G. M. Keyser, *Phys. Rev.* **81**, 602 (1951).

⁷ W. A. Wenzel and W. Whaling, *Phys. Rev.* **87**, 499 (1952).

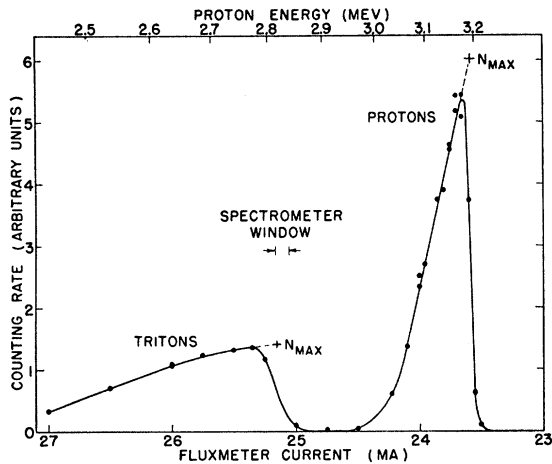


FIG. 1. Proton and triton spectrum obtained at $E_d=413$ kev. Spectrometer resolution $R_c=P/\Delta P=235$. The fluxmeter current is inversely proportional to the magnetic field. The proton energy scale refers to laboratory coordinates.

the protons and tritons after they had been deflected through 180° in the magnetic spectrometer.

Figure 1 shows a typical momentum spectrum of protons and tritons from the $d-d$ reaction for a bombarding energy of 413 kev. Momentum separation of the protons and tritons occurs because of the motion of the center of mass relative to the laboratory. We obtain the differential cross section $(d\sigma/d\Omega)$ at $\theta_{lab}=90.3^\circ$ from the formula of Snyder *et al.*⁸

$$4\pi d\sigma/d\Omega = N_{max}\epsilon_{eff}R_c/\Omega E_2q,$$

where N_{max} is obtained by extrapolating the trailing edge of the momentum spectrum to the midpoint of the leading edge, R_c and Ω are the spectrometer resolution and solid angle, respectively, q is the integrated target current in microcoulombs, E_2 is the energy in electron volts of the particles analyzed by the spectrometer, and $(d\sigma/d\Omega)$ is the differential cross section in millibarns per steradian. The effective stopping cross section, ϵ_{eff} , is related to the stopping cross sections ϵ_1 and ϵ_2 of the incident and emitted particle by the formula:

$$\epsilon_{eff} = \epsilon_1 dE_2/dE_1 + \epsilon_2 \cos\theta_1/\cos\theta_2.$$

Cross-section measurements with the spectrometer were not extended to energies below 200 kev because the large energy dependence of the cross section makes extrapolation of the trailing edge uncertain.

III. CROSS SECTION FROM THICK TARGET YIELD

The yield of protons from a thick D_2O ice target was measured at $\theta_{lab}=150^\circ$ for deuteron bombarding energies between 20.6 and 578 kev. Proportional counters were used to detect the protons. Three different counters were used in different geometrical

⁸ Snyder, Rubin, Fowler, and Lauritsen, Rev. Sci. Instr. 21, 852 (1950).

arrangements to check the consistency of the results. The thick target yield as a function of deuteron energy is shown in Fig. 2, the points plotted as circles and crosses show the excellent agreement between results taken with different counters with targets prepared from two different samples of D_2O . The differential cross section is given by $(d\sigma/d\Omega) = \epsilon dY(150^\circ)/dE_d$, where $Y(150^\circ)$ is the number of protons emitted into unit solid angle at $\theta_{lab}=150$ degrees for each deuteron incident on the thick target, and ϵ is the stopping cross section per deuterium atom in the target for deuterons of energy E_d . Methods of differentiation are discussed in Sec. VI, 10.

IV. ANGULAR DISTRIBUTION

For the angular distribution measurements a 7-inch diameter target chamber was constructed with windows 0.125 inch in diameter every 10° for θ_{lab} from 0° to 180° . The beam entered the window at 180° , and a quartz cover over the window at 0° served for alignment. The remaining windows were covered with 0.001-inch aluminum foil. The target holder was located accurately in the center of the chamber. A proportional counter fixed in position facing the 70° window was used as a monitor. A second counter, mounted on an arm which could be rotated about the center of the chamber, could be moved in front of any of the windows between 80° and 170° . A 4-inch diffusion pump under the chamber and a liquid nitrogen trap between the

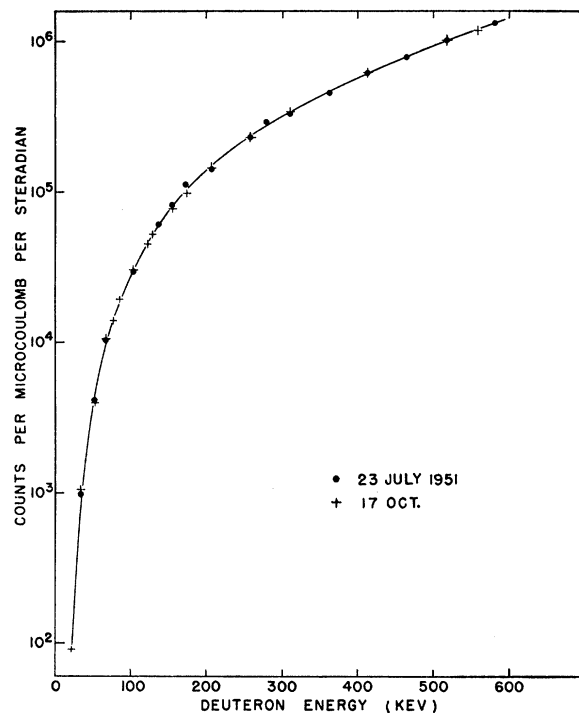


FIG. 2. Thick target yield of protons at $\theta_{lab}=150^\circ$. The solid circles were taken with the spectrometer target chamber and the crosses with the angular distribution target chamber. The energy scale refers to laboratory coordinates.

chamber and the pump maintained an operating pressure of 10^{-6} mm Hg in the chamber.

For deuteron energies above 200 keV the angular distribution was obtained with thin targets. A thin layer of ice was deposited on the cold target set at an angle of 45° to the incident beam. The ratio of the counting rate at an angle θ_{lab} to the rate at 70° measured with the monitor counter was obtained for θ_{lab} from 80° to 170° in 10° intervals. From the measured ratios and the kinetics of the reaction the angular distribution in the center-of-mass system was calculated. The effective energy at which the thin target yields were obtained was calculated in each case from the absolute thin target yield at 150° and the slope of the thick target yield at 150° as a function of energy

$$E_{eff} \approx E - \frac{1}{2} \frac{n(E_{eff}, 150^\circ)}{[dN(E, 150^\circ)/dE]_{E_{eff}}}$$

where $N(E, 150^\circ)$ is the thick target yield at 150° and bombarding energy, E , and $n(E_{eff}, 150^\circ)$ is the thin target yield at 150° . E_{eff} is the effective energy at which the angular distribution has been determined. The thickness of the targets used varied from 20 to 50 keV, and it was found that a given target varied less than 10 percent in thickness while measurements were being taken at all angles. The thin target angular yield as a function of energy and center-of-mass angle, normalized to a target of constant thickness, is plotted in Fig. 3.

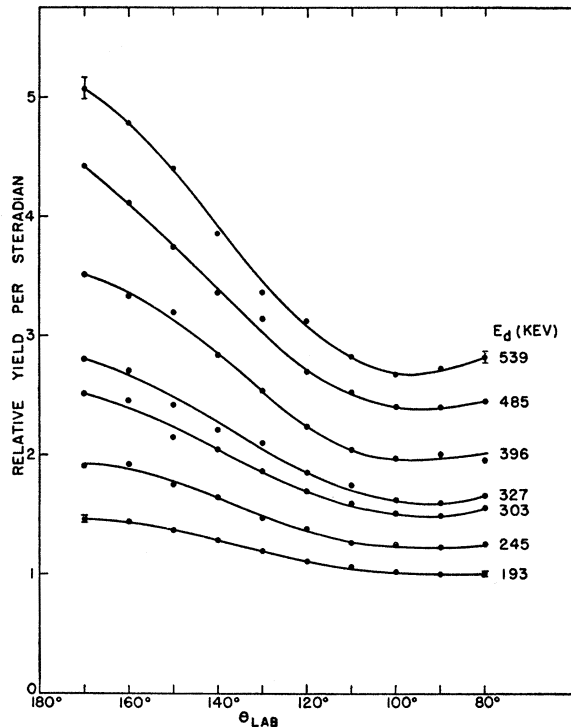


FIG. 3. The yield as a function of angle using thin ice targets at several bombarding energies. The yields are normalized to a fixed target thickness.

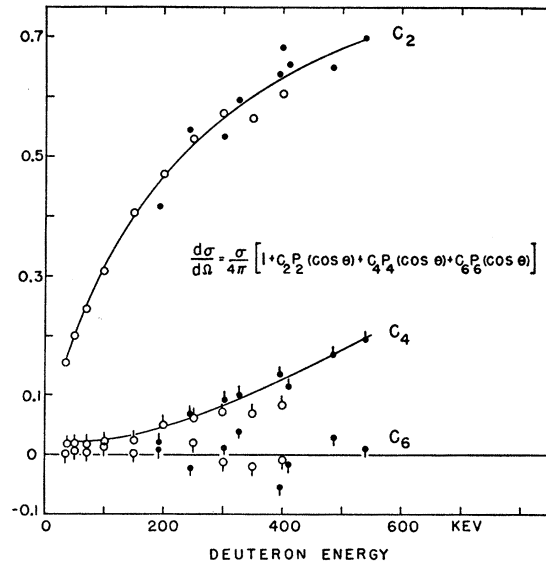


FIG. 4. D(d, p)T angular distribution. The solid circles were obtained from thin target yields and the open circles from thick target yields. Points with upward pointing tails refer to C_4 . Downward pointing tails refer to C_6 . The energy scale refers to laboratory coordinates.

The distribution for $\theta_{c.m.}$ between 90° and 180° is sufficient to determine the total angular distribution because of the symmetry of the reaction in the center-of-mass coordinates.

The rapid variation with energy of the cross section below 200 keV makes the thin target yield very sensitive to fluctuations in the target thickness. Therefore the angular distribution at low energies was obtained by differentiating with respect to energy the thick target yield curve at each angle to obtain the equivalent thin target yield. The thick target yield as a function of energy was expressed as the product of a barrier factor and a slowly varying function of energy and angle, $F(E_d, \theta_{lab})$. For each angle from 80° to 170° , the function $F(E_d, \theta_{lab})$ was determined from the ratio of the observed yield to the barrier factor. $F(E_d, \theta_{lab})$ was then plotted and differentiated graphically.

The angular distribution has been expanded in terms of Legendre polynomials. The variation of the coefficients in the expansion with energy is shown in Fig. 4. The solid points were obtained from thin target measurements, the open points from thick targets.

V. THE TOTAL CROSS SECTION

Knowing the cross section at one angle and the angular distribution, we have calculated the total cross section of the reaction. Figure 5 shows the results obtained in several ways. The points plotted as circles in Fig. 5 were obtained from the spectrometer measurements of $(d\sigma/d\Omega)$ at $\theta_{lab}=90.3^\circ$ and the angular distribution obtained by thin target methods. The points plotted as X's are based on the thick target yield at $\theta_{lab}=150^\circ$ and the thin target angular distribution. The

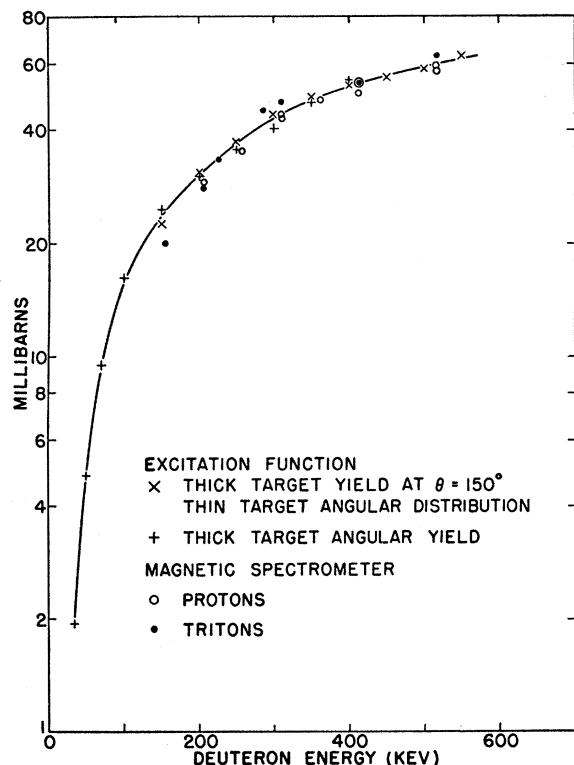


FIG. 5. Total cross section for the $D(d, p)T$ reaction. The energy scale refers to laboratory coordinates.

points plotted as plus signs show the integral over all angles of the differential cross section obtained by differentiating the thick target yield at each angle.

At high bombarding energies the cross section obtained from the thick target yield has been corrected for a small contribution from the $O^{16}(d, p)O^{17}$ reaction, since both of the proton groups from this reaction were counted along with the protons from the $d-d$ reaction. The cross sections have been measured for both $O^{16}(d, p)O^{17}$ proton groups with the magnetic spectrometer and are represented approximately by:

$$\text{Long-range group } -4\pi(d\sigma/d\Omega)_{90^\circ} = (0.5 \times 10^{10}/E_d) \times \exp(-355E_d^{-1/2}) \text{ millibarns,}$$

$$\text{Short-range group } -4\pi(d\sigma/d\Omega)_{90^\circ} = (1.2 \times 10^{10}/E_d) \times \exp(-355E_d^{-1/2}) \text{ millibarns,}$$

where E_d is the deuteron energy in the laboratory measured in keV. These values have been subtracted from the cross sections obtained from the thick target yield. We have assumed that the angular distribution for the $O^{16}(d, p)O^{17}$ reaction is spherically symmetric over the angular range investigated.

VI. DISCUSSION OF ACCURACY

1. Solid Angles

The solid angles for the various proportional counters were determined by direct measurement of the di-

ameter of the milled counter windows, 0.250 inch in diameter, and of the distance from the target to the counter window, which varied from 3.5 to 6.5 inches for the different counter arrangements. The solid angles determined by these measurements should be accurate to ± 2 percent.

The 0.125-inch diameter windows in the angular distribution chamber were smaller than the window in the counter outside the chamber so that the windows in the chamber determined the solid angle. The relative window size at each of the ten angles of observation from 80° to 170° was checked with a ThC' source at the target position. The average solid angle is known to within 1 percent, and the relative solid angles in the angular distribution chamber are known with somewhat higher accuracy.

The solid angle of the spectrometer was determined geometrically by the use of a known aperture at a measured distance from the target. The procedure is described in detail in reference 7. As an additional check, the proton spectrum obtained with the spectrometer was integrated to give the total yield of protons at 90.3° . This result was in excellent agreement with the total yield measured with the proportional counter set at $\theta_{lab} = 90^\circ$.

2. Current Integration

The current integrator was of conventional design using a condenser which was charged to a known voltage before being discharged by a fast relay. The integrator constant was determined under operating conditions by the use of a calibrated galvanometer. By a more accurate method, the integrator constant was obtained by means of batteries and precision resistors. The integrator constants obtained by the two methods of calibration agree within the experimental accuracy, and the integrator calibration is considered reliable within 2 percent.

3. Counter Efficiency

The pulse-height integral bias curve obtained with each proportional counter indicated an efficiency of 99 percent with a statistical uncertainty of ± 1 percent. The scintillation counter with the ZnS phosphor, which was used with the spectrometer to detect the reaction tritons and also for some of the proton spectra, was assumed to be 94 percent efficient, at the bias employed. This is the value measured in reference 7 for 500-keV protons. Comparison of the yield of 3 MeV protons taken first with the proportional counter and then with the scintillation counter attached to the spectrometer indicates that for these higher energy particles the efficiency of the scintillation counter may be nearer 92 percent. A 2-percent uncertainty is assigned to the value of the scintillation counter efficiency.

4. Target Contamination

The deuterium content of our heavy water was 99.8 percent according to the assay by the Stuart Oxygen Company. The liquid and its vapor were handled in an all-metal system. Reaction yields were reproducible over a period of three months and after refilling the liquid reservoir. Target contamination by the incident deuteron beam would tend to increase the relative concentration of deuterium in the target. If we assume that the incident particles are deposited over a volume equal in cross section to the size of the beam spot and in depth to the range of the bombarding particles, we find that for 50-keV deuterons a contamination of the order of +1 percent would exist after 1000 microcoulombs of bombardment. If the deuterons tend to collect on the surface of the target, a more serious error in measured yield would be expected. By replenishing the target surface frequently, we have sought to avoid such surface contamination. No time dependent increase in yield which might be attributed to this effect was ever observed.

5. Beam Contamination

A comparison of the reaction yields from the monoatomic, diatomic, and triatomic ions indicated that the beam contamination was low. The DD⁺ and the DDD⁺ yields were regularly somewhat higher than the D⁺ yield, but this effect never exceeded 3 percent and seemed to be independent of energy. Contamination of the D⁺ beam by the HH⁺ ion would not be expected to produce even this effect if it resulted from the ½ percent impurity in the supply to the ion source. Presumably the somewhat larger contamination comes from the production of H₂ gas from oil vapor and the gaskets. In another check on beam contamination the magnitude of the H⁺ beam was found to be of the order of 1 percent of the D⁺ beam under the same generator operating conditions.

6. Energy Scale

Correct calibration and linearity of the energy scale are very important because of the critical energy dependence of the cross section at low energy. Calibration and linearity measurements of the generator voltage are described in reference 7. The good agreement between the D⁺, DD⁺, DDD⁺ yields at corresponding individual deuteron energies is taken as further evidence for the linearity of the generator voltage scale.

7. Secondary Electron Emission

The target was maintained at a potential of 300 volts positive with respect to the surrounding chamber to suppress the emission of secondary electrons from the target. Between the last beam defining slit and the target was placed a ring-shaped electrode through which the beam passed. This ring was held at 180 volts nega-

TABLE I. D(*d, p*)H³ total cross section and angular distribution.

$$\frac{d\sigma}{d\Omega} = \frac{\sigma_T}{4\pi} [1 + C_2 P_2(\cos\theta) + C_4 P_4(\cos\theta) + C_6 P_6(\cos\theta) + \dots].$$

<i>E</i> (keV)	$\frac{\sigma_T}{4\pi}$ millibarns	<i>C</i> ₂	<i>C</i> ₄
35	1.94	0.155	0.02
50	4.81	0.195	0.02
70	9.49	0.247	0.02
100	15.8	0.310	0.023
150	23.8	0.400	0.031
200	30.6	0.470	0.045
250	37.0	0.523	0.052
300	43.1	0.566	0.080
350	48.1	0.601	0.103
400	52.3	0.632	0.126
450	55.8	0.660	0.150
500	59.0	0.684	0.175
550	62.0	0.704	0.203

tive with respect to the surrounding chamber walls to prevent secondary electrons knocked out of the slits from reaching the target.

8. Beam Neutralization

The effect of beam neutralization was measured by deflecting the beam magnetically in the 60-cm tube between the electrostatic analyzer and the target chamber. The magnet was located 5 cm from the target chamber. With the beam coming through the analyzer, the ratio of the D(*d, p*)T yields with the beam on the target and deflected away from the target gives a direct measurement of the percentage of neutralization. With the normal operating pressure of 1.0×10⁻⁶ mm of Hg in the target chamber and 4×10⁻⁶ mm of Hg in the tube between the analyzer and the target chamber, the neutralization measured was 0.7 percent. When air was admitted to the analyzer, raising the ion gauge pressures to 5.0×10⁻⁶ in the target chamber and 2.5×10⁻⁵ mm of Hg in the connecting tube, the measured neutralization was 3 percent. These measurements were made at 51.5 keV; measurements of the neutralization at lower energies was not feasible because of the low yields. However, Bartels⁹ and Keene¹⁰ have found that the electron capture cross section of protons in hydrogen increases by less than a factor of two when the bombarding energy decreases from 25 to 17.5 keV. These energies correspond to 50 and 35 keV, respectively for bombarding deuterons. Kanner¹¹ finds that the capture cross section in air is of the same order of magnitude as in hydrogen. On the basis of these results we have made no correction for beam neutralization.

9. Beam Intensity

Evaporation of the ice target occurred if the beam power became too large. To determine whether this effect was important, the DD⁺ current on a ⅛-inch diameter target spot was varied from 0.3 μa to 1.8 μa

⁹ H. Bartels, Ann. Physik **13**, 373 (1932).

¹⁰ J. P. Keene, Phil. Mag. **40**, 369 (1949).

¹¹ H. Kanner, Phys. Rev. **84**, 1211 (1951).

at a bombarding energy of 103 kev. There was no observable difference in yield.

10. Statistical Uncertainty and Differentiation

The statistical uncertainty in the individual experimental points varies from 1 to 3 percent for the thick target measurements, and from 1 to 4 percent for the thin target results. The error introduced in the differentiation has been minimized by the method of differentiation. At low energies we expect the cross section to have the approximate form: $\sigma(E) \propto E^{-1} \exp(-44.4 E^{-3})$, and the stopping cross section: $n^{-1}(dE/dX) \propto E^{\frac{1}{2}}$, where E is in kev. Hence the thick target yield is given approximately by $N(E_0) \propto \int_0^{E_0} dE E^{-3} \exp(-44.4 E^{-3}) \propto \exp(-44.4 E^{-3})$. For each angle we have plotted $F(E, \theta) = N(E, \theta) \exp(44.4 E^{-3})$ and differentiated $F(E, \theta)$ with respect to the energy. The quantity dN/dE is then found from $dN(E, \theta)/dE = \exp(-44.4 E^{-3}) [dF(E, \theta)/dE + 22.2 F(E, \theta) E^{-3}]$. $F(E, \theta)$ is a smoothly varying function of energy and the differentiation can be carried out accurately. Moreover, in the differentiation of $N(E, \theta)$, the term containing F is much larger than the one containing dF/dE . Hence, at low energies, it is felt that the errors introduced by differentiation are not significant.

In the energy range 100–500 kev it was found that the total yield varied approximately as E^2 . A plot of $N(E, \theta)$ vs E^2 yielded more consistent values for $dN(E, \theta)/dE$ than either of two semilog plots tried. At energies above 150 kev the differentiation introduces some uncertainty into the measured cross section and angular distribution. An estimate of the amount of this uncertainty may be obtained from the difference in angular distribution and cross section obtained by the use of thin target and thick target techniques. From Fig. 5, for example, the difference in cross section is seen to be of the order of a few percent in the energy range $E_d = 150$ to 400 kev.

11. Stopping Cross Section

Since the experiment measures the ratio of the reaction cross section to the stopping cross section, ϵ , the uncertainties in the measurement of ϵ , described in reference 7, appear in our value for the reaction cross section. It is significant that certain possible systematic errors cancel out when the stopping cross section and reaction cross-section experiments are considered together. For example, an error in the integrator constant would produce a corresponding error in the calculated

values of ϵ , but not in the $D(d, p)T$ cross section. An error in the spectrometer constant R_c/Ω , would directly affect ϵ , but not the reaction cross section obtained with the spectrometer. In fact, the spectrometer has effectively measured the ratio of the $D(d, p)T$ reaction cross section to the $O^{16}(p, p)O^{16}$ scattering cross section. Here we have assumed that the ratio $\epsilon(D_2O)/\epsilon(\text{air})$ is the same for protons of 500 kev and 3 Mev. However, since $d\epsilon_{\text{eff}}/d\epsilon(\text{air}) \approx \frac{1}{3}$, small variations in the assumed stopping power of D_2O are not significant. Values for $\epsilon(\text{air})$ were obtained from the literature.¹² The stopping cross section for reaction tritons is obtained from reference 7.

12. Probable Error

The largest contribution to the probable error is the 4 percent uncertainty in the value of $\epsilon(D_2O)$. If the $D(d, p)T$ cross section were based on the thick target yield alone, additional errors due to solid angle, counter efficiency, target and beam contamination, energy calibration, neutralization, and statistics would raise the probable error to slightly over 5 percent. However, the partial cancellation of systematic errors from the spectrometer measurements tends to reduce the error. The good agreement of the spectrometer results, using both protons and tritons, with the results from the thick target excitation function is significant. Thus we have assigned a probable error of 5 percent to the values of the total cross section listed in Table I. These values were taken from the solid curve drawn through the experimental points in Fig. 5.

VII. COMPARISON WITH OTHER MEASUREMENTS

The thick target yield is about 25 percent lower than that obtained by Bretscher *et al.*² using the same technique. No explanation for this discrepancy can be offered. Agreement with Moffatt *et al.*⁴ and with Arnold *et al.*⁵ in the low energy region is within 5 percent, and the agreement with McNeill and Keyser⁶ in the middle energy range is good. Regarding the angular distribution, the agreement with the results of Bretscher *et al.*, and of Moffatt *et al.*, is good, although the finite amount of $P_4(\cos\theta)$ which we find makes exact comparison difficult.

One of the authors (WAW) would like to express his appreciation to the Eastman Kodak Company for a fellowship given to him during the course of the work described in this paper.

¹² H. A. Bethe, *Revs. Modern Phys.* **22**, 213 (1950).